Analysis of Flow and Heat Transfer Over an External Boundary Covered With a Porous Substrate

P. C. Huang[1] and K. Vafai[1,2]

Nomenclature

C_f = friction coefficient, Eq. (22)
C_T = total friction coefficient, Eq. (23)
$c_{p,f}$ = fluid heat capacity, $W\ s\ kg^{-1}\ K^{-1}$
Da_L = Darcy number = K/L^2
F = a function used in expressing inertia terms
H = thickness of the porous medium, m
k = thermal conductivity, $Wm^{-1}\ K^{-1}$
K = permeability of the porous medium, m^2
L = length of the external boundary as shown in Fig. 1(*a*), m
P = pressure, Pa
r = ratio of x-component interfacial velocity to free-stream velocity = u_I/u_∞
Pr = Prandtl number = ν/α
Re_L = Reynolds number = $u_\infty L/\nu$
T = temperature, K
u = x-component velocity, ms^{-1}
v = y-component velocity, ms^{-1}
x = horizontal coordinate, m
y = vertical coordinate, m
α = thermal diffusivity, m^2s^{-1}
α_{eff} = effective thermal diffusivity = $k_{eff}/\rho_f c_{p,f}$, m^2s^{-1}
δ = boundary-layer thickness, m
δ_t = thermal boundary-layer thickness, m
ϵ = porosity of the porous medium
Λ_L = inertial parameter = $FL\ \epsilon/\sqrt{K}$
μ = dynamic viscosity, $kgm^{-1}s^{-1}$
ν = kinematic viscosity, m^2s^{-1}
ρ = fluid density, kgm^{-3}
τ_w = wall shear stress, Nm^{-2}

Superscripts

$\bar{}$ = dimensionless quantity

Subscripts

eff = effective
f = fluid
I = interface
P = porous
t = thermal
w = condition at the wall
x = local
∞ = condition at infinity

Introduction

During the past decade there has been a renewed research interest in fluid flow and heat transfer through porous media due to its relevance in various applications such as drying processes, thermal insulation, direct contact heat exchangers, heat pipes, filtration, etc. Comprehensive reviews of the existing studies on these topics can be found in Cheng (1978) and Tien and Vafai (1989).

An important problem related to convection through porous media is flow and heat transfer through composite porous systems. The convection phenomenon in these systems is usually affected by the temperature and flow field interactions in the porous space and the open space. This type of composite system is encountered in many applications, such as some solidification problems, crude oil extraction, thermal insulation, and some geophysical systems. Due to the mathematical difficulties in simultaneously solving the coupled momentum equations for both porous and fluid regions, it is usually assumed that there is only one fluid-saturated porous region (i.e., there is no fluid region and interfacial surface) and the flow is through this infinitely extended uniform medium. Thus the interaction between the porous-saturated region and the fluid region did not form a part of most of these studies. In addition, most of the existing studies deal primarily with the mathematical formulations in the porous medium based on the use of Darcy's law, which neglects the effects of a solid boundary and inertial forces. These assumptions will easily break down since in most applications the porous medium is bounded and the fluid velocity is high.

Inertial and boundary effects on forced convection along a flat plate embedded in a porous medium were studied by Vafai and Tien (1981, 1982), and Vafai et al. (1985). Among these studies Vafai and Tien (1981) treated a fluid-saturated porous medium as a continuum, integrated the momentum equation over a local control volume, and derived a volume-averaged momentum equation, which included the flow inertia as well as the boundary effects. There have been few investigations related to porous/fluid composite systems. Poulikakos (1986) presented a detailed numerical study of the buoyancy-driven flow instability for a fluid layer extending over a porous substrate in a cavity heated from the bottom. Another related problem is that of Poulikakos and Kazmierczak (1987). In that work a fully developed forced convection in a channel that is partially filled with a porous matrix was investigated and the existence of a critical thickness of the porous layer at which the value of Nusselt number reaches a minimum was demonstrated. Kaviany (1987), Beckermann and Viskanta (1987), and Nakayama et al. (1990) evoked the boundary layer approximations and solved the generalized momentum equation presented by Vafai and Tien (1981) to investigate the same flow configuration. Vafai and Kim (1990) performed a numerical analysis of forced convection over a porous/fluid composite system, which consisted of a thin porous substrate attached to the surface of the flat plate.

The primary objective of this study is to present an analytical solution for forced convection boundary layer flow and heat transfer through a composite porous/fluid system and thereby provide a comprehensive yet extremely fast alternative as well as a comparative base for numerical solutions addressing these type of interfacial transport. The details of the interaction phenomena occurring in the porous medium and the fluid layer are systematically analyzed, revealing the effects of various parameters governing the physics of the problem under consideration. The present analysis drastically reduces typical CPU times for the interfacial simulations presented by Vafai and Kim (1990). It should be noted that the configuration considered in this work is quite generic and forms an important and fundamental geometry for a variety of applications.

Theory

The flow configuration and the coordinate system for this problem are shown in Fig. 1(*a*). In this study, we are assuming that the flow is steady, two dimensional, and that the boundary

[1]Department of Mechanical Engineering, The Ohio State University, Columbus, OH 43210.
[2]Professor, Fellow ASME.
Contributed by the Heat Transfer Division of THE AMERICAN SOCIETY OF MECHANICAL ENGINEERS. Manuscript received by the Heat Transfer Division September 1992; revision received September 1993. Keywords: Forced Convection, Materials Processing and Manufacturing Processes, Porous Media. Associate Technical Editor: C. E. Hickox, Jr.

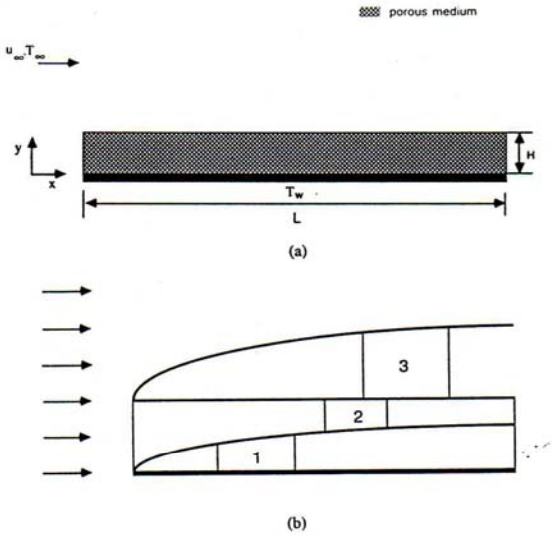

Fig. 1 *(a)* **Schematic diagram of the flow over an external boundary with an attached porous substrate; (*b*) control volume for integral momentum analysis of (1) porous boundary layer, (2) interfacial region between the porous and fluid layers, and (3) the fluid boundary layer**

layer approximations hold (this was established by Vafai and Kim, 1990). The conservation equations, which include the boundary and inertial effects, in the porous region can then be written as (Vafai and Tien, 1981):

$$\frac{\partial u_P}{\partial x_P}+\frac{\partial v_P}{\partial y_P}=0 \tag{1}$$

$$u_P\frac{\partial u_P}{\partial x_P}+v_P\frac{\partial v_P}{\partial y_P}=-\frac{1}{\rho}\frac{\partial P_P}{x_P}-\frac{\nu_{\text{eff}}}{K}u_P-\frac{F\epsilon}{\sqrt{K}}u_p^2+\nu_{\text{eff}}\frac{\partial^2 u_P}{\partial y_p^2} \tag{2}$$

$$u_P\frac{\partial T_P}{\partial x_P}+v_P\frac{\partial T_P}{\partial y_P}=\alpha_{\text{eff}}\frac{\partial^2 T_P}{\partial y_p^2} \tag{3}$$

where all the variables and parameters are defined in the nomenclature section. Note that variables u, v, and T are volume-averaged quantities. Since at a sufficiently large distance from the wall the flow field is uniform, the free-stream axial pressure gradient in the porous region required for maintaining the x-component interfacial velocity u_I can be expressed as

$$-\frac{1}{\rho}\frac{dP}{dx_P}=-\frac{\nu_{\text{eff}}}{K}u_I-\frac{F\epsilon}{\sqrt{K}}u_I^2-u_I\frac{du_I}{dx_P} \tag{4}$$

Inserting Eq. (4) into Eq. (2), the momentum equation becomes

$$u_P\frac{\partial u_P}{\partial x_P}+v_P\frac{\partial u_P}{\partial y_P}=\frac{\nu_{\text{eff}}}{K}(u_I-u_P)+\frac{F\epsilon}{\sqrt{K}}(u_I^2-u_P^2)+\nu_{\text{eff}}\frac{\partial^2 u_P}{\partial y_P^2}+u_I\frac{du_I}{dx_P} \tag{5}$$

In the fluid region, the conservation equations for mass, momentum, and energy are

$$\frac{\partial u_f}{\partial x_f}+\frac{\partial v_f}{\partial y_f}=0 \tag{6}$$

$$u_f\frac{\partial u_f}{\partial x_f}+v_f\frac{\partial u_f}{\partial y_f}=-\frac{1}{\rho}\frac{\partial p_f}{\partial x_f}+v_f\frac{\partial^2 u_f}{\partial y_f^2} \tag{7}$$

$$u_f\frac{\partial T_f}{\partial x_f}+v_f\frac{\partial T_f}{\partial y_f}=\alpha_f\frac{\partial^2 T_f}{\partial y_f^2} \tag{8}$$

The boundary conditions are

$$x<0:\quad u=u_\infty,\quad P=P_\infty \tag{9}$$

$$x>0,\quad y=0:\quad u=v=0 \tag{10}$$

$$x>0,\quad y\to\infty:\quad u=u_\infty,\quad P=P_\infty \tag{11}$$

This implies that the free-stream flow field is not affected by the presence of the porous media. This was found to be a very good assumption based on the analysis presented by Vafai and Kim (1990). The matching conditions at the interface of the porous/fluid system are

$$u|_{y=H^-}=u|_{y=H^+},\quad v|_{y=H^-}=v|_{y=H^+} \tag{12a}$$

$$P|_{y=H^-}=P|_{y=H^+},\quad \mu_{\text{eff}}\frac{\partial v}{\partial y}\bigg|_{y=H^-}=\mu_f\frac{\partial v}{\partial y}\bigg|_{y=H^+} \tag{12b}$$

$$\mu_{\text{eff}}\left(\frac{\partial u}{\partial y}+\frac{\partial v}{\partial x}\right)\bigg|_{y=H^-}=\mu_f\left(\frac{\partial u}{\partial y}+\frac{\partial v}{\partial x}\right)\bigg|_{y=H^+} \tag{12c}$$

$$T|_{y=H^-}=T|_{y=H^+},\quad k_{\text{eff}}\frac{\partial T}{\partial y}\bigg|_{y=H^-}=k_f\frac{\partial T}{\partial y}\bigg|_{y=H^+} \tag{12d}$$

It should be noted that here we are not trying to resolve a philosophical and complex question with respect to the physical nature of the interface. In reality, a fluid–fluid or porous–fluid interface is more complicated than what has been modeled by investigators both in porous–fluid and fluid–fluid interface modeling. Here we have adopted the traditional mathematical idealization used for both fluid–fluid or porous–fluid interfaces, i.e., representing the interface by a singular surface.

Analysis

An integral analysis is applied to three different regions: the porous boundary layer region, the fluid boundary layer within the porous substrate, and the fluid boundary layer outside of the porous substrate as shown in Fig. 1(*b*).

Integral Momentum Equation for the Porous Boundary Layer. Following the Karman–Pohlhausen integral method, the parabolic velocity distribution is described as

$$\frac{u_P}{u_I}=2\frac{y_P}{\delta_P}-\left(\frac{y_P}{\delta_P}\right)^2 \tag{13}$$

where δ_P is the thickness of the momentum boundary layer in the porous region. After a lengthy analysis the integral momentum equation in dimensionless form for the porous region is derived as

$$\frac{3}{5}\bar{\delta}_P r\frac{dr}{d\bar{x}_P}+\frac{2}{15}r^2\frac{d\bar{\delta}_P}{d\bar{x}_P}=-\frac{r\bar{\delta}_P}{3\text{Re}_L\text{Da}_L}-\frac{7}{15}\Lambda_L r^2\bar{\delta}_P+\frac{2r}{\text{Re}_L\bar{\delta}_P} \tag{14}$$

where

$$\bar{x}=\frac{x}{L},\quad \bar{\delta}_P=\frac{\delta_P}{L},\quad r=\frac{u_I}{u_\infty}\text{ and }\text{Re}_L=\frac{u_\infty L}{\nu_{\text{eff}}},$$

$$\text{Da}_L=\frac{K}{L^2},\quad \Lambda_L=\frac{FL\epsilon}{\sqrt{K}}$$

This equation is subject to the following initial condition given by $\bar{\delta}_P(0)=0$, $r(0)=0$. It should be noted that $x_f=x_P$. However, we have used separate notations for x_f and x_P for the sake of consistency.

Integral Momentum Equation for the Fluid Boundary Layer Within the Porous Substrate. A lengthy integral analysis for the control volume 2 shown in Fig. 1(*b*) leads to the momentum integral equation for that region

$$-\frac{1}{\rho}\left(\delta_f\frac{\partial P}{\partial x_f}+\tau_I\right)=\frac{\partial}{\partial x_f}\int_0^{\delta_f}u_f(u_\infty-u_f)dy_f$$

$$-(1-r)u_\infty^2\left[\frac{1}{3}r\frac{d\delta_P}{dx_P}-\left(H-\frac{1}{3}\delta_P\right)\frac{dr}{dx_P}\right] \quad (15)$$

where τ_I is the shear stress in the porous/fluid interface and δ_P and δ_f are the thicknesses of porous and fluid momentum boundary layers, respectively. Assuming the following parabolic velocity distribution for the fluid boundary layer:

$$\frac{u_I}{u_\infty}=r+(2-2r)\frac{y_f}{\delta_f}-(1-r)\left(\frac{y_f}{\delta_f}\right)^2 \quad (16)$$

where the subscript f refers to fluid and $r=u_I/u_\infty$. Substituting Eq. (16) into Eq. (15) and replacing τ_I by $\nu_f(\partial u_f/\partial y_f)_{y_f=0}$, the derived integral momentum equation in dimensionless form becomes

$$\left(\frac{2}{15}+\frac{r}{15}-\frac{r^2}{5}\right)\frac{d\bar{\delta}_f}{d\bar{x}_f}+\bar{\delta}_f\left(\frac{1}{15}-\frac{2r}{5}\right)\frac{dr}{d\bar{x}_f}=(2-2r)\frac{1}{\mathrm{Re}_L\bar{\delta}_f}+(1-r)$$

$$+(1-r)\left[\frac{1}{3}r\frac{d\bar{\delta}_P}{d\bar{x}_f}+\left(\frac{\bar{\delta}_P}{3}-\bar{H}\right)\frac{dr}{d\bar{x}_f}\right] \quad (17)$$

where

$$\bar{x}_f=\frac{x_f}{L},\quad \bar{\delta}_f=\frac{\delta_f}{L},\quad \bar{\delta}_P=\frac{\delta_P}{L}\text{ and }\bar{H}=\frac{H}{L},\quad \mathrm{Re}_L=\frac{u_\infty L}{\nu_f}$$

This equation is subject to $\bar{\delta}_P(0)=0$, $\bar{\delta}_f(0)=0$, $r(0)=0$.

Integral Momentum Equation for the Fluid Boundary Layer Outside of the Porous Substrate. A similar procedure for the control volume 3 in Fig. 1(*b*), which incorporates the interfacial boundary conditions, leads to the integral momentum equation for the interfacial region

$$\nu_f\frac{\partial u_f}{\partial y_f}+\nu_{\mathrm{eff}}u_I(x)[H-\delta_P(x)]+\frac{F\epsilon}{\sqrt{K}}\left(\frac{u_I}{u_\infty}\right)^2(H-\delta_P(x))=0 \quad (18)$$

Substituting the velocity distributions for both porous and fluid boundary layers into Eq. (19) gives the dimensionless form of the integral momentum equation

$$\frac{2(1-r)}{\mathrm{Re}_L\bar{\delta}_f}+\frac{(\bar{H}-\bar{\delta}_P)r}{\mathrm{Re}_L\mathrm{Da}_L}+\Lambda_L r^2(\bar{H}-\bar{\delta}_P)=0 \quad (19)$$

This equation is subject to $\bar{\delta}_P(0)=0$, $\bar{\delta}_f(0)=0$, $r(0)=0$.

Integral Energy Equation. Since only one thermal boundary layer was observed in the forced convection through the porous/fluid composite system under consideration (Vafai and Kim, 1991), in this study the control volume 1 in Fig. 1(*b*) is used to derive the integral energy equation, which depends on the relative values of δ_P and δ_f. Performing an energy balance over control volume 1 and using the following parabolic temperature distribution:

$$\theta=\frac{T_P-T_w}{T_\infty-T_w}=2\frac{y_P}{\delta_t}-\left(\frac{y_P}{\delta_t}\right)^2 \quad (20)$$

the integral energy equation in dimensionless form is obtained after a very lengthy analysis for three different possible conditions as

$$\left(\frac{\bar{\delta}_t}{3}-\frac{\bar{\delta}_P}{3}+\frac{\bar{\delta}_P^2}{6\bar{\delta}_t}-\frac{\bar{\delta}_P^3}{30\bar{\delta}_t^2}\right)\frac{dr}{d\bar{x}_P}$$

$$+\frac{r}{3}\left[\left(1+\frac{\bar{\delta}_P}{10\bar{\delta}_t}-\frac{\bar{\delta}_P^2}{2\bar{\delta}_t^2}\right)\frac{d\bar{\delta}_t}{d\bar{x}_P}-\left(1-\frac{\bar{\delta}_P}{\bar{\delta}_t}+\frac{3\bar{\delta}_P^2}{10\bar{\delta}_t^2}\right)\frac{d\bar{\delta}_P}{d\bar{x}_P}\right]$$

$$\frac{d\bar{\delta}_P}{d\bar{x}_P}=\frac{2}{\mathrm{Pr}_{\mathrm{eff}}\mathrm{Re}_L}\frac{1}{\bar{\delta}_t}\quad \delta_t>\delta_P \quad (21a)$$

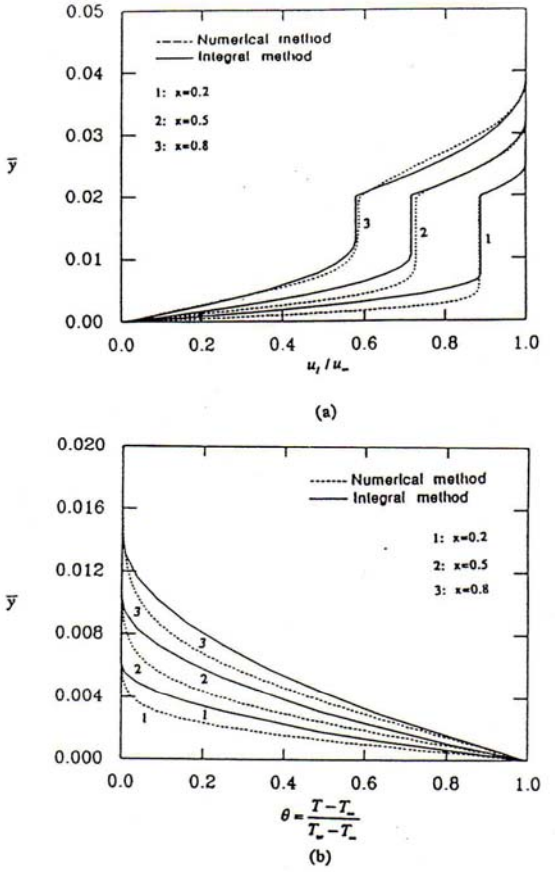

Fig. 2 (*a*) Velocity and (*b*) temperature distribution along the flat plate at three different locations, x = 0.2, 0.5, and 0.8, for $\mathrm{Re}_L=3\times10^5$, $\Lambda_L=0.35$, $\mathrm{Da}_L=8\times10^{-6}$, Pr = 0.7 $k_{\mathrm{eff}}/k_f=1$, $H/L=0.02$

$$\frac{1}{3}\left(\bar{\delta}_t\frac{dr}{d\bar{x}}+r\frac{d\bar{\delta}_t}{d\bar{x}}\right)=\frac{2}{\mathrm{Pr}_{\mathrm{eff}}\mathrm{Re}_L\bar{\delta}_t}\quad \delta_t=\delta_P \quad (21b)$$

and

$$\left(\frac{\bar{\delta}_t^2}{6\bar{\delta}_P}-\frac{\bar{\delta}_t^3}{30\bar{\delta}_P^2}\right)\frac{dr}{d\bar{x}_P}+r\left[\left(1+\frac{\bar{\delta}_t}{3\bar{d}_P}-\frac{\bar{\delta}_t^2}{10\bar{\delta}_P^2}\right)\frac{d\bar{\delta}_t}{d\bar{x}_P}\right.$$

$$\left.-\left(\frac{\bar{\delta}_P^2}{6\bar{\delta}_t^2}-\frac{\bar{\delta}_t^3}{15\bar{\delta}_P^3}\right)\frac{d\bar{\delta}_P}{d\bar{x}_P}\right]=\frac{1}{\mathrm{Pr}_{\mathrm{eff}}\mathrm{Re}_L}\frac{1}{\bar{\delta}_t}\quad \delta_t<\delta_P \quad (21c)$$

This equation is subject to $\bar{\delta}_P(0)=0$, $\bar{\delta}_f(0)=0$, $r(0)=0$.

Discussion of Results and Conclusions

The combinations of Eqs. (15), (17), (19), and (21) form a set of four nonlinear simultaneous ordinary differential equations for the four unknowns δ_P, δ_f, δ_t, and r. The fourth-order Runge-Kutta method is applied to solve these equations.

As discussed earlier, the present analysis is extremely effective and expedient in showing the physics of the interfacial transport. In what follows, the solutions obtained by integral analysis are examined and compared with the velocity and temperature distributions obtained by Vafai and Kim (1990). Figure 2 shows how the boundary layer thickness, the velocity and temperature distributions are affected by the presence of a porous matrix. The results in Fig. 2 are presented for Reynolds number of $\mathrm{Re}_L=3\times10^5$, Darcy number $\mathrm{Da}_L=8\times$

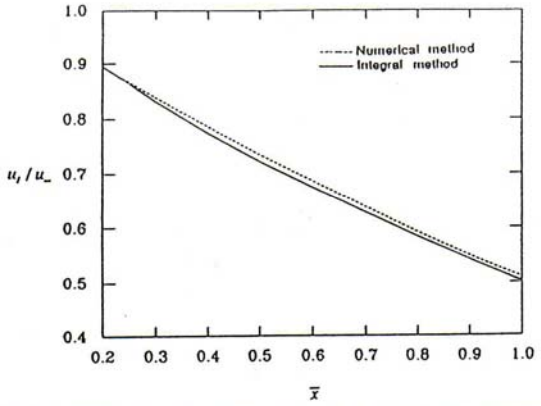

Fig. 3 Comparison of the integral solutions with numerical solutions for x-component interfacial velocity along the flat plate for $\Lambda_L = 0.35$, $Re_L = 3 \times 10^5$, $Da_L = 8 \times 10^{-6}$, $H/L = 0.02$

10^{-6}, inertial number $\Lambda_L = 0.35$, Prandtl number Pr = 0.7, effective conductivity ratio $k_{eff}/k_f = 1$, and the dimensionless thickness of the porous slab of $\overline{H} = 0.02$. As expected, there are two distinct momentum boundary layers: one in the porous region and the other one in the fluid region. Inside the porous region as the transverse coordinate increases, the velocity profile is shown to increase from zero to a constant value, which is maintained until the outer boundary layer appears. Once it crosses the porous/fluid interface, it goes through a smooth transition and approaches a free-stream value in the fluid region.

As expected, the momentum boundary layers in the porous medium as well as in the fluid region grow in the streamwise direction. Consequently, the magnitude of the interfacial velocity decreases to adapt to this growth. Figure 2(*b*) shows the temperature distribution along the flat plate at three different locations. The values of the thickness of the thermal boundary layer obtained by integral method are larger than those obtained by numerical method. This is due to the approximate expressions used for the velocity and temperature profiles in the integral analysis. Figure 3 compares the results of the numerical method and the integral method in the streamwise direction for the interfacial velocity. The results show a remarkably good agreement between the integral analysis and the full numerical solution considering the complexity and the much larger CPU requirements for the numerical simulations. It should be noted that the type of agreements found in Figs. 2(*a*), 2(*b*), and 3 are typical for a wide range of pertinent parameters but are not presented here for the sake of brevity.

The configuration considered in this work is quite generic and forms an important and fundamental geometry for a variety of applications. The results given in this work present a comprehensive yet easy comparative base for numerical solutions addressing this type of interfacial transport. The present analysis provides a rather *accurate simulation* of the interfacial transport *while drastically reducing* previously reported computational times by Vafai and Kim (1990) for this type of simulations.

References

Beckermann, C., and Viskanta, R., 1987, "Forced Convection Boundary Layer Flow and Heat Transfer Along a Flat Plate Embedded in a Porous Medium," *Int. J. Heat Mass Transfer*, Vol. 30, pp. 1547–1551.

Cheng, P., 1978, "Heat Transfer in Geothermal System," *Adv. Heat Transfer*, Vol. 14, pp. 1–105.

Kaviany, M., 1987, "Boundary Layer Treatment of Forced Convection Heat Transfer From a Semi-infinite Flat Plate Embedded in Porous Media," ASME JOURNAL OF HEAT TRANSFER, Vol. 109, pp. 345–349.

Nakayama, A., Kokudai, T., and Koyama, H., 1990, "Non-Darcian Boundary Layer Flow and Forced Convective Heat Transfer Over a Flat Plate in a Fluid-Saturated Porous Medium," ASME JOURNAL OF HEAT TRANSFER, Vol. 112, pp. 157–162.

Poulikakos, D., 1986, "Buoyancy-Driven Convection in a Horizontal Fluid Layer Extending Over a Porous Substrate," *Phys. Fluids*, Vol. 29, pp. 3949–3957.

Poulikakos, D., and Kazmierczak, M., 1987, "Forced Convection in a Duct Partially Filled With a Porous Material," ASME JOURNAL OF HEAT TRANSFER, Vol. 109, pp. 653–662.

Tien, C. L., and Vafai, K., 1989, "Convective and Radiative Heat Transfer in Porous Media," *Adv. Appl. Mech.*, Vol. 27, pp. 225–281.

Vafai, K., and Tien, C. L., 1981, "Boundary and Inertia Effects on Flow and Heat Transfer in Porous Media," *Int. J. Heat Mass Transfer*, Vol. 24, pp. 195–203.

Vafai, K., and Tien, C. L., 1982, "Boundary and Inertia Effects on Convective Mass Transfer in Porous Media," *Int. J. Heat Mass Transfer*, Vol. 25, pp. 1183–1190.

Vafai, K., Alkire, R. L., and Tien, C. L., 1985, "An Experimental Investigation Heat Transfer in Variable Porosity Media," ASME JOURNAL OF HEAT TRANSFER, Vol. 107, pp. 642–647.

Vafai, K., and Kim, S. J., 1990, "Analysis of Surface Enhancement by a Porous Substrate," ASME JOURNAL OF HEAT TRANSFER, Vol. 11, pp. 700–705.

Perturbation Solution for Laminar Convective Heat Transfer in a Helix Pipe

G. Yang[1] and M. A. Ebadian[1,2]

Introduction

Coiled pipes are used extensively in many industries. A general study of flow and heat transfer in the toroidal pipe (the coiled pipe with negligible pitch) has been reviewed by Berger et al. (1983) and Shah and Joshi (1987). It has long been recognized that the pitch of the coiled pipe will create an additional rotational force known as torsion. In a coiled pipe with considerable pitch, torsion will distort the symmetric loops of the secondary flow and twist the axial velocity contours (Wang, 1981; Germano, 1989; Kao, 1987; Tuttle, 1990). To distinguish, coiled pipes with a substantial pitch are defined as helicoidal pipes. Although numerous studies have been conducted on the toroidal pipe, a literature survey indicates that only a few papers have been published to study convection heat transfer in the helicoidal pipe (Manlapaz and Churchill, 1981; Futagami and Aoyama, 1988. In these papers, the overall heat transfer behavior has been studied by simplifying the governing equations. However, none have discussed the effects of torsion on the temperature distribution and peripheral heat transfer rate in the helicoidal pipe, which is very important information for the effective design of the compact heat exchanger and combustor. The purpose of this note is to summarize the analytical results of both thermally and hydrodynamically fully developed convective heat transfer in a helicoidal pipe subject to the (H1) boundary condition.

[1]Department of Mechanical Engineering, Florida International University, Miami, FL 33199.

[2]Fellow ASME, corresponding author.

Contributed by the Heat Transfer Division of THE AMERICAN SOCIETY OF MECHANICAL ENGINEERS. Manuscript received by the Heat Transfer Division July 1993; revision received February 1994. Keywords: Augmentation and Enhancement, Forced Convection, Heat Exchangers. Associate Technical Editor: Y. Jaluria.